

## Morphological & physical characteristics of Ceria (CeO<sub>2</sub>) doped Zirconia Toughened Alumina (ZTA) ceramics composites

Bipin Kumar Singh<sup>a,\*</sup>, A. Selvarasu<sup>b</sup>, P. Ganesan<sup>a</sup> and K. Raja<sup>c</sup>

<sup>a</sup>Centre for Augmented Intelligence and Design, Department of Mechanical Engineering, Sri Eshwar College of Engineering, Coimbatore - 641202, Tamil Nadu, India

<sup>b</sup>Department of Mechanical Engineering, V.S.B. Engineering College, Karur-639111, Tamil Nadu, India

<sup>c</sup>Department of Mechanical Engineering, Anna University Regional Campus Coimbatore, Coimbatore- 641046, Tamil Nadu, India

Zirconia Toughened Alumina (ZTA) composites are widely used in both emerging and established industries due to their high hardness, excellent wear resistance, and high hot hardness. However, their inherent brittleness limits their applications, which can be addressed by incorporating softer phases inside hard ceramic matrices. Hence, in this study, different weight percentages of CeO<sub>2</sub> (ranging from 0 to 20 wt.%) as soft phases were added to ZTA matrices to investigate the resulting changes in microstructure, phase transitions, and physical properties. Investigation starts with synthesis of ZTA/CeO<sub>2</sub> obeying co-precipitation method. After development of composites morphological evaluation i.e. XRD & FESEM for all samples were thoroughly carried out. The analysis indicated continuous increase in tetragonal phases of zirconia with incorporation of CeO<sub>2</sub> particles, strongly supporting the transformation toughening phenomenon. The maximum hardness obtained as 15.19 GPa, for 5 wt.% CeO<sub>2</sub>, whereas, maximum toughness obtained as 5.73 MPa.m<sup>1/2</sup> for 20 wt.% CeO<sub>2</sub>. The decrement with higher percentage of CeO<sub>2</sub> attributed to the formation of larger grain size and porosity inside the composites. In addition, the transform toughening phenomenon also contributed to improvement in physical properties especially toughness of the composites.

**Keywords:** Ceria (CeO<sub>2</sub>), Zirconia Toughened alumina (ZTA), Hardness and fracture toughness.

### Introduction

Zirconia toughened alumina (ZTA) ceramics are advanced composite materials that combine the high hardness and wear resistance of alumina (Al<sub>2</sub>O<sub>3</sub>) with the improved fracture toughness imparted by the addition of zirconia (ZrO<sub>2</sub>) [1,2]. The zirconia particles dispersed within the alumina matrix undergo a stress-induced phase transformation (transform toughening phenomenon) under mechanical load, which helps to inhibit crack propagation and significantly enhances the material's toughness [3,4]. This makes ZTA ceramics especially valuable in applications where both hardness and resistance to cracking are critical. Furthermore, the tremendous applications like cutting tools, orthopedic implants such as femoral heads in hip replacements, wear-resistant components in pumps and valves, and ballistic armor attract the composites for scientific studies. ZTA ceramics offer a balanced combination of strength, durability, and chemical stability, making them suitable for demanding environments across medical, industrial,

and defence sectors. Researchers also observed that the physical properties of ZTA could further extend by incorporation of some soft additives like CeO<sub>2</sub>, CuO, MoS<sub>2</sub>, Graphene and MXene [5-8]. In this regard, Tan et al. [9] selected different percentage of CeO<sub>2</sub> reinforced inside the ZTA matrices to evaluate physical properties. Researchers selected powder metallurgy route obeying spark plasma sintering process to develop all the composites. Investigation showed 5 wt.% CeO<sub>2</sub> inside ZTA govern highest physical properties i.e. hardness (1688 HV) and fracture toughness (9.91 MPa.m<sup>1/2</sup>). The improvement was attributed to the stress-induced phase transformation toughening.

Earlier investigation suggested that in zirconia-toughened alumina, the transformation toughening mechanism plays a key role in enhancing toughness. This mechanism relies on the stress-induced phase transformation of metastable zirconia particles, which is most effective near the tip of a growing crack. Earlier studies (Zeng et al., 2004) [10] have shown that zirconia undergoes a phase transformation from monoclinic to tetragonal at approximately 1170 °C, with further heating leading to the formation of a cubic phase around 2370 °C that persists up to the melting point. When zirconia is cooled from processing

\*Corresponding author:  
Tel : +91 8392006007  
E-mail: bipinmech2008@gmail.com

temperatures to room temperature, the tetragonal phase can be retained in a metastable state due to the presence of stabilizing oxides such as yttria [11], ceria [12], or magnesia [13]. These stabilizers prevent the complete transformation to the monoclinic phase during cooling. However, under critical stress, the metastable tetragonal phase can still transform into the monoclinic phase, resulting in a volumetric expansion of about 3–5% and a shear strain of around 16%. This stress-induced transformation creates compressive stresses around the crack tip, effectively resisting crack growth and thereby significantly improving the fracture toughness of the ceramic matrix. Al-Amin et al. [14] showed higher content of YSZ approx. 15 wt.% with 5 wt% CeO<sub>2</sub> can able to achieved fracture toughness of 12.03 MPa. m<sup>1/2</sup> at sintering temperature of 1500 °C. Whereas, the highest value hardness (14.15 GPa) was achieved with 5 wt.% YSZ with 5 wt.% CeO<sub>2</sub> at 1450 °C. Again, phase transformation mechanism along with formation of larger grains were the possible cause to improve the toughness. Azhar et al. [15] studied the effect of different percentage of CeO<sub>2</sub> inside ZTA-TiO<sub>2</sub> ceramics in terms of physical and microstructural behaviour changes. Researchers revealed that the higher average grain intercept (AGI) value was responsible for decrement in grain sizes up to 5 wt.% addition of CeO<sub>2</sub>, further addition increases the grain size. The formation of highest secondary phases i.e. Zr<sub>0.4</sub>Ti<sub>0.6</sub>O<sub>2</sub> with incorporation of 5 wt.% addition of CeO<sub>2</sub> corresponding to the improvement in toughness as well as hardness. Similar type of experiments was carried out by Bakhtierkhalzi et al. [16] in which different percentage of TiO<sub>2</sub> (0–4 wt.%) was doped in (5 wt.%) CeO<sub>2</sub>/ZTA matrices. Researchers noticed 1.5 wt% TiO<sub>2</sub> composite had superior physical properties attributed to the formation of lowest grain size of alumina. Further addition of TiO<sub>2</sub> showed the presence of Al<sub>2</sub>TiO<sub>5</sub> phases that accelerates the grain size of alumina particles, result in porous and less dense structure, reflected on lower value of hardness.

Extensive research on evaluation of physical and functional properties of CeO<sub>2</sub>/ZTA/TiO<sub>2</sub> composites was carried out by Eggidi and his colleagues [17,18]. Researchers reported a hardness of 1650 ± 9.6 HV10 and toughness of 8.45 ± .14 MPa.m<sup>1/2</sup> with incorporation of 4 wt.% TiO<sub>2</sub> into CeO<sub>2</sub>/ZTA matrices. Said composition also showed minimum coefficient of friction (COF) i.e. 0.32 at load of 50 N, as well as highest wear resistance properties, corresponding to finer grain size and tetragonal stability. Very recent, Ganeshan et al. [19] showed significant improvement in COF i.e. 24.45% compared to parent matrix with incorporation of 5 wt.% CeO<sub>2</sub> inside ZTA matrices. Stable tetragonal and transformation toughening phenomenon synergistically diminished the grain sizes responsible for improvement in functional properties. Imariouane et al. [20] investigated the impact resistance properties enhanced by incorporation of yttria and ceria doped inside Zirconia

matrices. Finding illustrated that the t-m transformation significantly affects impact resistance (highest in case of maximum transformability of phases), highest govern by Ce-TZP composite (high transformation ability) followed by 1.5Y-TZP, and then 3Y-TZP. Shan et al. [21] demonstrated the biomedical potential of Ce-ZTA as a bone implant material, highlighting enhanced cell proliferation achieved through the reinforcement of cerium oxide. Research also emphasized cerium oxide's ability to promote bone-implant integration and stimulate new bone formation.

Very recent, Abbas and his colleague [22] examined the effects of CeO<sub>2</sub> doping (0–1 wt%) on alumina-toughened zirconia (ATZ) ceramics sintered in the range of 1250–1500 °C to evaluate mechanical properties. The optimal densification (~92.1%) was achieved with 0.2 wt% CeO<sub>2</sub> at 1500 °C. Microstructural analysis revealed fine, equiaxed grains with no secondary phases and uniform Ce distribution. Research also showed that the vickers hardness increased with CeO<sub>2</sub> addition and temperature, peaking at 12.18 GPa for 0.2 wt% CeO<sub>2</sub> due to refined grains and reduced porosity. Hydrothermal aging (180 °C, 10 bar, 100 h) showed that CeO<sub>2</sub> significantly suppressed the tetragonal-to-monoclinic transformation i.e. monoclinic content decreased from ~31.7% (undoped) to ~9.6% (0.2 wt% CeO<sub>2</sub>). Gavalda-Diaz et al. [23] highlighted the recent advances in toughening ceramics through microstructural engineering, focusing on Ceramic Matrix Composites (CMCs), zirconia-based ceramics, and novel bioinspired or nanostructured approaches that enhance crack resistance and pseudo-ductile behavior. Despite ceramics' inherent brittleness, innovations such as transformation toughening, fibre-matrix interfaces, and nacre-inspired designs have significantly improved their toughness, bringing them closer to reliable, damage-tolerant materials for aerospace, biomedical, and energy applications.

Hence, from above literature, it is clear that the ceria particles crucially affect the physical and functional properties of ZTA. The improvement in physical and functional properties is attributed to the t-m transformation showed by earlier researchers, but the stability of tetragonal phases with increasing percentage of ceria is not discussed by any researchers. Therefore, this research selects (0–20 wt.%) of ceria inside the ZTA matrices in order to evaluate the physical and functional properties. The evaluation of functional properties in terms of coefficient of friction for high percentage of ceria particle is still not carried out by any researcher. The investigation begins with a morphological evaluation, followed by an assessment of physical properties such as density, hardness, and toughness. Subsequently, the physics laid behind the improvement of physical properties for the developed composites are thoroughly examined with increasing concentrations of ceria particles. This study also emphasizes the advantageous effects of plate-like second-phase particles embedded within the ZTA matrix.

Furthermore, a correlation has been established between the microstructure of the developed composites and their physical properties.

### Synthesis of Powders and Preparation of Samples

In this investigation, coprecipitation route has been selected to develop all composites as it provides a uniform distribution of different components inside the matrices (better homogeneous structure) with better phase formation. The earlier literature [24] suggested that coprecipitation enables uniform distribution of dopant ions at the atomic scale within the zirconia matrix. Furthermore, the coprecipitation route uses low-cost inorganic salts and simpler processing steps, making it more scalable and industrially viable while, other preparation methods like sol-gel, which requires expensive alkoxide precursors and often involves complex hydrolysis-condensation reactions. Hydrothermal synthesis, obviously provide excellent for producing highly crystalline and morphology-controlled nanoparticles, typically requires high-pressure autoclaves and extended reaction times, limiting its cost-effectiveness and large-scale applicability which are absent in coprecipitation route. Additionally, coprecipitation generally results in lower residual organics compared to sol-gel, minimizing porosity and improving sinterability of ceramic composites. So, in this method, requisite amount of chemicals (i.e. Aluminium nitrate, Yttrium nitrate and Zirconyl nitrate) is dissolved in distilled water to form solution. The developed transparent solution is further mixed with dilute  $\text{NH}_4\text{OH}$  (0.1 mol. %) during stirring condition, in order to form precipitate. The precipitates are completely formed when pH of solution reached  $\approx 9$ , maintaining a temperature around 70-80 °C to restrict the agglomeration of precipitate. After complete formation of precipitate the stirring process is continue for 2-3 hr maintaining 70-80 °C. hr. After stirring the solution is ideally kept for 12 hr then decant in a filter unit. In filter unit, continuous warm water is poured on the precipitate till complete removal of nitrate ions takes place ( $\text{pH} \approx 9$ ). After removal of nitrate ions, the precipitated are collected in a petri dish, followed by placing in a oven at temperature 100 °C for 24hr. The dried lumps are collected from petri dish, followed by crushing in wet media (like acetone) using mortar pestle. The crushed powders are calcined at 800 °C using high temperature furnace. After calcination, the powders are mixed with cerium oxide  $\text{CeO}_2$  (Aldrich) using a planetary ball milled (alcoholic media with alumina balls having 8-12 mm diameter) based on requisite weight percentage (0-20 wt.%). After mixing the powders are dried in an oven and again decomposed at 1400 °C for 2 hr in order to form all phases present in the composites.

The well dried powders of composites are used for preparation of samples, which is in square shape of 12 ×

12 (L × B) mm having 8mm thickness. The preparation of samples are starts with pouring of requisite amount of fine powder in a die, which is pressed on hydraulic press using suitable punch. The pressing of samples was carried out uniaxially at a pressure of 5 ton.cm<sup>-2</sup>. The pressed green samples are slowly ejected from the die-punch arrangement, followed by sintering process at high temperature of 1600 °C for 2 hr. The sintered samples are mirror polished using silicon carbide powder followed by diamond paste on Bain polisher. Before polishing the phases analysis and morphological study of all the samples are carried out using XRD and FESEM technique. In XRD evaluation the detector-angle range ( $2\theta$ ) starts from 20° and ends with 70°. Furthermore, the tetragonal phases developed inside the samples are calculated using XRD techniques based on earlier article published by Singh et al. [25]. The phases are calculated with high focused to analyse the transformation toughening mechanism. After XRD analysis, the FESEM images of all samples are taken at same magnification for better comparison of grain sizes.

After morphological evaluation the polished samples are used to evaluate the physical and functional properties. At first, the bulk density of all the samples is calculated using Archimedes principle. The micro hardness of all samples is calculated through Vickers hardness (Model: BV:120). Ten readings are taken for each samples, four at the corners and six at the different positions in middle of the samples. Average of same is shown as evaluated value of hardness. The indentation toughness is also calculated through Vickers hardness testing machine at a load of 5 N. The process to evaluate the indentation toughness is based on earlier published work of Raja et al. [26]. In case of toughness evaluation, six readings are taken for each sample, four at the corners and two at the middle. The average of same is cited in the result.

## Results and Discussions

### Morphological characteristics

The investigation, starts with evaluation of phases through XRD technique for all samples sintered at 1600 °C. The XRD graphs of developed composites are compiled on a single abscissa as shown in Fig. 1 for better understanding. The tetragonal and monoclinic (m-ZrO<sub>2</sub> and t-ZrO<sub>2</sub>) phases, plays crucial role in stress-induced toughing mechanism are precisely calculated using XRD plots and shown thorough bar chart in Fig. 2(a). The evaluated crystal sizes for all composites developed in this investigation are shown in Fig. 2(b). From the XRD plots and bar charts, a significant influence of  $\text{CeO}_2$  particles is observed on t-ZrO<sub>2</sub> phases of zirconia.

From XRD analysis a continuous increment in peak intensity for tetragonal phase of zirconia is observed with increasing amount of ceria inside ZTA. The adverse effect is observed on monoclinic phases. The evaluated value of t-ZrO<sub>2</sub> and m-ZrO<sub>2</sub> also support similar finding. The

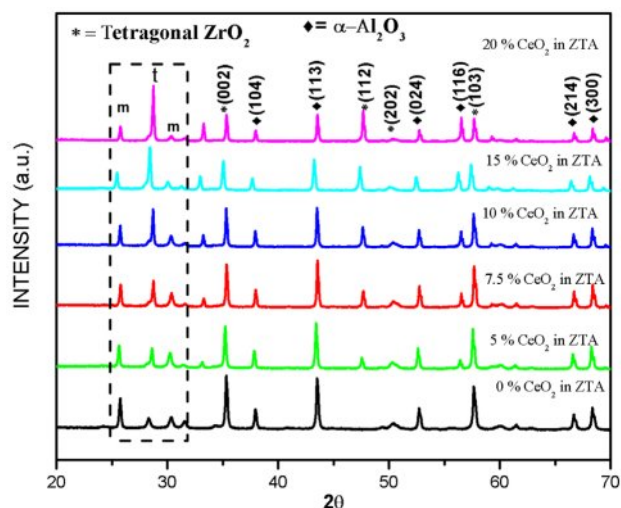


Fig. 1. XRD of all composites  $\text{CeO}_2$  doped ZTA.

increasing trend of tetragonal phases is also replicated on the crystal size, which is monotonically increasing with increasing percentage of ceria in ZTA. The results are in-line with earlier investigation of Sato and Shimada [27] and Tsukuma [28]. Researchers noticed that the improvement in retention of metastable tetragonal phases at room temperature is attributed to presence of ceria particles. Hence, from finding it can be concluded that the ceria particles significantly enhance the percentage of tetragonal phases inside the cluster of ZTA matrix.

The structural analysis for all developed composites is carried out through FESEM images, maintaining same magnification during capturing the images. The FESEM images of all composites are shown in Fig. 3. Well dispersed ceria grains inside the cluster of ZTA with high homogeneous structure is observed for all the composites with EDS is shown in Fig. 4. The EDX analysis shown in Fig. 4 suggests that the ceria particle

possess a plate like structure. The observation from all FESEM images suggests that the grain sizes of ceria increase with increasing weight percentage of ceria inside the ZTA cluster. The similar observation is also noticed through grain size measurement using particle size analyser i.e. grain sizes of composites increases with increasing percentage of ceria inside the cluster same is shown in Fig. 5(a). From Fig. 5(a) an increment from 1.26 micron to 1.68 micron is observed, corresponding to the presence of ceria molecules that supports the fusion of grains inside the cluster. Similar kind of observation was earlier reported by Tsukuma and Shimada [29]. Researchers noticed that the presence of  $\text{CeO}_2$  formed a pyrochlore type compound that break the lattice constants of the tetragonal phases. The lattice constrain breakdown creates higher percentage of tetragonal phases inside the ZTA matrix also stated in XRD analysis, reflects an increase in grain size of composites. Therefore, it can be concluded that the presence of ceria increases the overall grain sizes of composites as well as tetragonal phases of zirconia inside the cluster of ZTA matrices. The FESEM images also suggests homogeneous distribution of all elements inside the cluster of ZTA, indicates high densification of composites after sintering. A detailed study on the thermal stability for ceria particles is explored by Shelyug et al. [30]. Researcher demonstrated that Ceria ( $\text{CeO}_2$ ) is a key stabilizer for zirconia ( $\text{ZrO}_2$ ) because it promotes retention of the metastable tetragonal phase at room temperature, which is essential for transformation toughening. The solubility limit of  $\text{CeO}_2$  in  $\text{ZrO}_2$  typically ranges from 12 to 16 mol%, although the exact value can depend on processing conditions, sintering temperature, and the presence of other dopants. Within this solubility range,  $\text{Ce}^{4+}$  ions substitute for  $\text{Zr}^{4+}$  in the lattice, introducing lattice strain that stabilizes tetragonal domains and inhibits premature tetragonal-to-monoclinic transformation. Furthermore, some investigation [31, 32] also revealed that at optimal doping

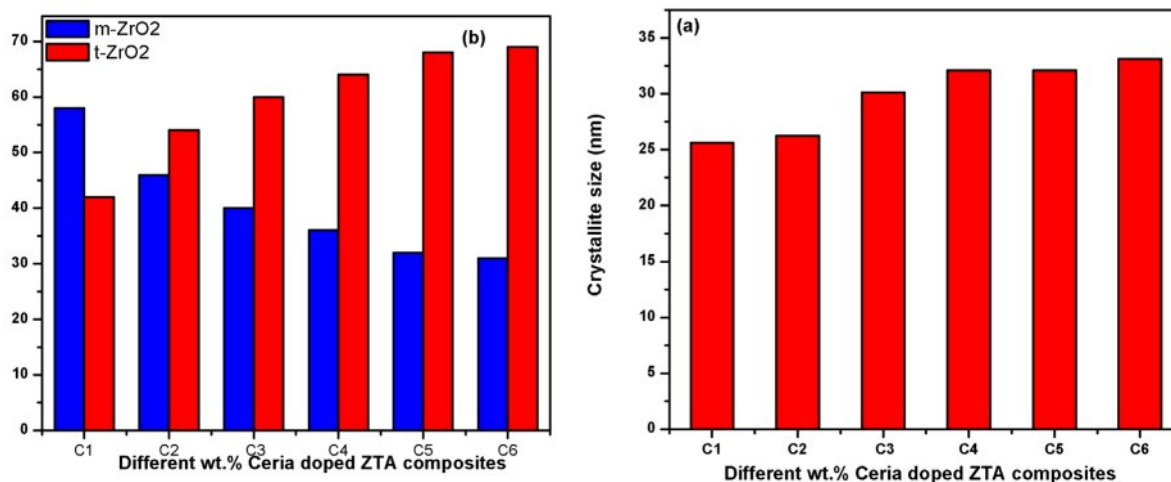


Fig. 2. (a) m- $\text{ZrO}_2$  and t- $\text{ZrO}_2$  phases of zirconia with different composites (b) Crystallite sizes evaluated for all composites.



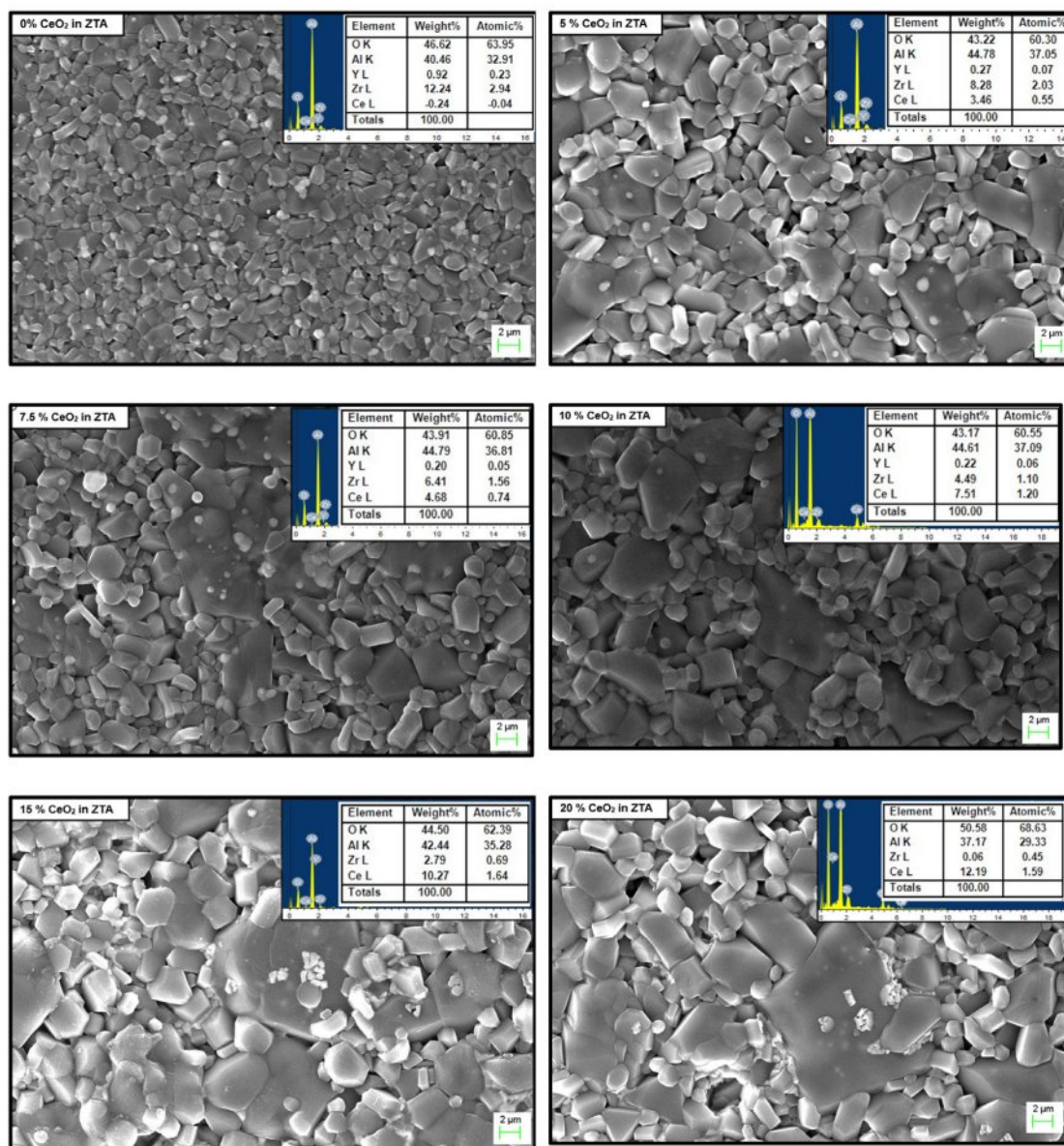


Fig. 3. Structure analysis of different wt.% of CeO<sub>2</sub> (FESEM image with EDAX).

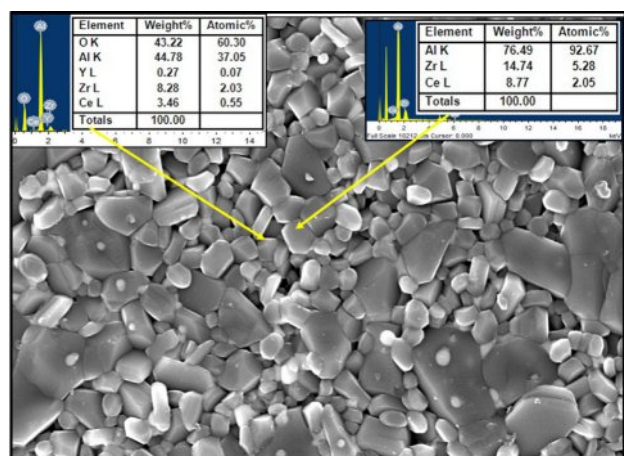


Fig. 4. EDS and FESEM of 5 wt.% CeO<sub>2</sub>/ZTA.

levels (usually 10–12 mol%), zirconia maintains its tetragonal phase even under prolonged thermal exposure or hydrothermal aging, minimizing low-temperature degradation (LTD). Higher ceria contents can lead to formation of a cubic phase, which is stable but lacks transformation toughening, potentially reducing fracture toughness. Conversely, lower CeO<sub>2</sub> levels may not fully stabilize tetragonal grains, making them susceptible to spontaneous transformation over time.

### Physical characteristics

The analysis on physical characteristic starts with calculation of bulk density using Archimedes principal using kerosene media. All calculated values are summarized in Fig. 6(b). The analysis reveal stagnated value of bulk density up to 5 wt.% of ceria followed by

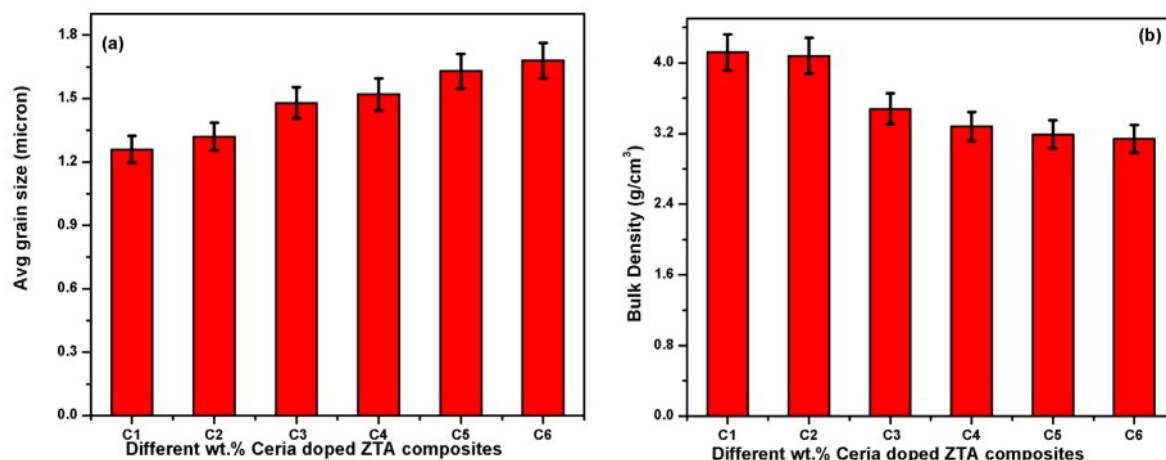


Fig. 5. (a) Evaluated values of average grain size (b) Calculated values of bulk density.

monotonically decrement up to 20 wt.%. This happened due to increase in grain size with higher content of ceria inside the cluster. The higher grain size probably increases the porosity or voids inside the matrix, reflects on decrement in bulk density [33].

After analysis of bulk density, the micro hardness and indentation toughness for all composites are evaluated on Vickers hardness tester. The evaluated values of hardness and toughness are summarized through bar chart in Fig. 6(a) and (b).

From Fig. 5(a) an interesting result has been noticed i.e. hardness value increased for 5 wt.% Ceria (i.e. 15.19 GPa), stagnant in case 7.5 wt.% of ceria followed by monotonically decrement in hardness value. The earlier extensive study carried out by Rejab et al. [33] also postulated similar trend of result. Literature suggested that the pores size and shape with distribution of additives (homogeneous) inside the cluster crucially affect the value of hardness. Hence, better densification

with homogeneous structure of grains possible improve the hardness value for light quantity of ceria. Further increase in percentage of ceria hinder the grain size result in abnormal porosity increment responsible for decrement in hardness value. Another factor i.e. formation of  $\text{Ce}_2\text{Zr}_3\text{O}_{10}$  (a soft particle) generally formed with higher content of ceria showed by Rejab et al. [34] also contributed for the significant decrement in hardness value with high percentage of ceria.

The calculated values of indentation fracture toughness are compiled in Fig. 6(b) that suggest monotonically increment in values with increasing percentage of ceria inside the ZTA cluster. Earlier researches on toughness suggested that larger grain size (enhance porosity), presence of soft particle and transformation toughening phenomenon (i.e. better retention of metastable tetragonal  $\text{ZrO}_2$ ) crucially affect the value of fracture toughness of composites. The analysis on XRD clearly revealed that the retention of metastable tetragonal phases of  $\text{ZrO}_2$

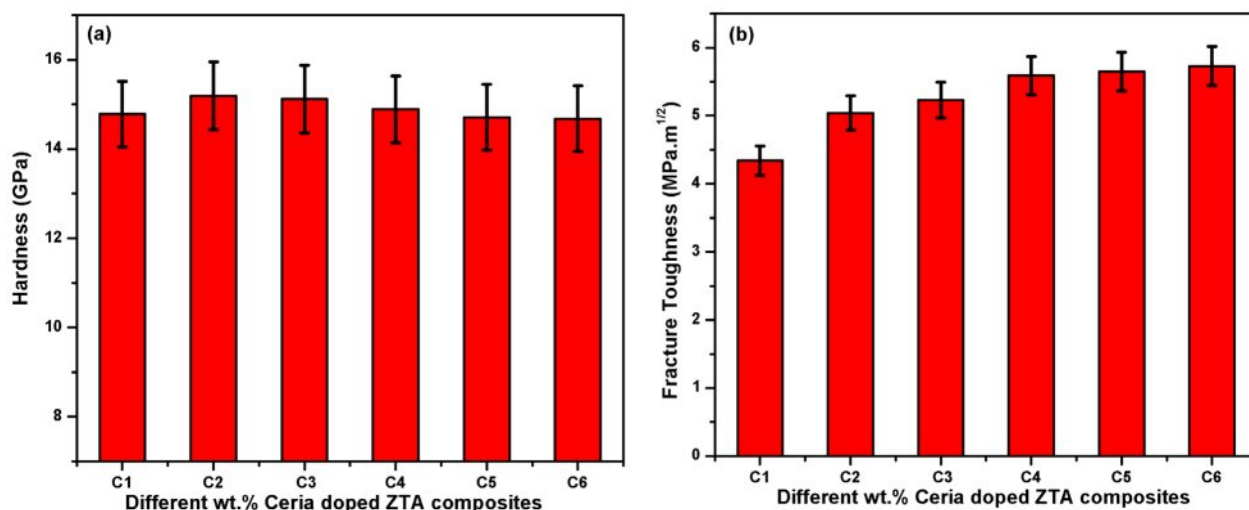


Fig. 6. (a) Vicker hardness (b) Indentation Fracture Toughness.

are higher with high amount of ceria due to good solid solubility of  $\text{Ce}^{4+}$  ions. The presence of high amount of metastable tetragonal  $\text{ZrO}_2$  crucially affect the toughness of bulk composites as its volume expands during transformation of tetragonal to monoclinic at critical stress [35,36]. The expansion in volume ( $\sim 3\text{-}5\%$ ) restrict the propagation of crack or act as energy barrier inside the cluster require higher energy for further propagation of crack responsible for continuous improvement in toughness. The said mechanism i.e. transformation toughening phenomenon combined with softer particles ( $\text{Ce}_2\text{Zr}_3\text{O}_{10}$ ) and larger grain sizes creates favourable condition for high value of toughness to  $5.73 \text{ MPa.m}^{1/2}$  at high percentage of ceria. Therefore, it can be concluded that the presence of low quantity of ceria favourably enhance the hardness and fracture toughness, whereas higher content of ceria improves the toughness at cost of hardness value.

### Conclusion

Well densified ceria doped zirconia toughness alumina ceramics composites are developed to evaluate the morphological and physical characteristics. The morphological study reveals continuous increment in retention of metastable tetragonal phases i.e. good solubility of  $\text{Ce}^{4+}$  ions with zirconia ions with increasing percentage of ceria inside ZTA cluster. The FESEM images shows continuous increment in grain sizes (formation of  $\text{Ce}_2\text{Zr}_3\text{O}_{10}$ ) with increasing quantity of ceria. 5 wt.% Ce-ZTA, shows higher hardness value (15.19 GPa) due to better densification, consequences of homogeneous grain size inside the cluster. Higher porosity and presence of softer particle inside the cluster decreases the value of hardness with higher percentage of ceria. The larger grain size, presence of soft particle and transformation toughening phenomenon combinedly improve the toughness value to  $5.73 \text{ MPa.m}^{1/2}$ . Hence, lighter percentage of ceria in ZTA matrix could be beneficial for improvement in physical properties due to homogeneous structure and better densification.

### Acknowledgement

The authors are thankful to Principal and Director of SECE for allowing the facilities and support during experimentation.

### Funding:

Fund received by DST-INDIA-FIST Program-2022 [TPN-83971] (SR/FST/College-/2022/1300).

### Conflicts of interest/Competing interests

Authors don't have any conflict.

### Availability of data and material

Data are available in the manuscript.

### References

1. B.K. Singh, Trans. Indian Ceram. Soc. 82[1] (2023) 1-13.
2. A. Pratap, B.K. Singh, and N. Sardana, Mater. Today: Proc. 66 (2022) 3738-3742.
3. S.K. Gautam and B.K. Singh, Mater. Chem. Phys. 25 (2023) 128813.
4. B.K. Singh, K. Ghosh, S.S. Roy, B. Mondal, and N. Mandal, Trans. Indian Ceram. Soc. 77[4] (2018) 219-225.
5. G. Gokilakrishnan, B.K. Singh, and M. Vigneshkumar, J. Ceram. Process. Res. 24[4] (2023) 655-661.
6. B.K. Singh, A. Kumar, R. Cep, A. Kumar, A. Kumar, N. Dogra, and K. Logesh AIP Adv. 14[8] (2024) 085207.
7. P. Ganeshan, T. Rajesh, B.K. Singh, and K. Raja, J. Ceram. Process. Res. 25[6] (2024) 931-936.
8. B.K. Singh, R. Singh, Y.H. Ahn, and S. Samanta, J. Ind. Eng. Chem. 148 (2025) 329-344.
9. P. Tan, Y. Yang, Y. Sui, and Y. Jiang, Ceram. Int. 46[6] (2020) 7510-7516.
10. D. Zeng, N. Katsube, and W.O. Soboyejo, Mech. Mater. 36[11] (2004) 1057-1071.
11. K. Raja, P. Ganeshan, B.K. Singh, R.K. Upadhyay, P. Ramshankar, and V. Mohanavel, Sādhanā 48[2] (2023) 72.
12. M. Nawa, S. Nakamoto T. Sekino, and K. Niihar, Ceram. Int. 24[7] (1998) 497-506.
13. P. Kumar, A. Pratap, N. Mandal, and B.K. Singh, Mater. Today: Proc. 44 (2021) 1806-1810.
14. M. Al-Amin, H.T. Mumu, S. Sarker, M.Z. Alam, and M.A. Gafur, J. Korean Ceram. Soc. 60[1] (2023) 141-154.
15. A.Z. A.Azhar, S.H.M. Shawal, H. Manshor, A.M. Ali, N.A. Rejab, E.C. Abdullah, and Z.A. Ahmad, J. Alloys Compd. 773 (2019) 27-33.
16. M. Bakhtierkhalzi, M.W. Islam, M. Suzaudhin, M.N. Islam, and A. Al Mahmood, Ceram. Int. 49[4] (2023) 6666-6670.
17. O. Eggidi and A.K. Pandey, Int. J. Appl. Ceram. Tec. 20[1] (2023) 294-305.
18. O. Eggidi and A.K. Pandey, J. Asian Ceram. Soc. 11[3] (2023) 385-394.
19. P. Ganeshan, Y. Sravani, K. Raja, and B.K. Singh, J. Ceram. Process. Res. 24[5] (2023) 781-787.
20. M. Imariouane, M. Saâdaoui, N. Labrador, H. Reveron, and J. Chevalier, Ceramics 8[1] (2025) 26.
21. J. Shan, S. Wang, H. Xu, H. Zhan, Z. Geng, H. Liang, and M. Dai, J. Biomater. Appl. 36[6] (2022) 976-984.
22. M. Abbas, T.A. Mare, L. Ghazal, S. Makeen, R. Mohamed, and M. Al-Ejji, Nanoscale 17 (2025) 22248-22259.
23. O. Gavalda-Diaz, E. Saiz, J. Chevalier, and F. Bouville, Int. Mater. Rev. 70[1] (2025) 3-30.
24. P. Ramanujam, B. Vaidhyanathan, J. Binner, A. Anshuman, and C. Spacie Ceram. Int. 40[3] (2014) 4179-4186.
25. B.K. Singh, B. Mondal, and N. Mandal, Ceram. Int. 42[2] (2016) 3338-3350.
26. K. Raja, M. Dhanabal, B.K. Singh, and P. Ganeshan, J. Ceram. Process. Res. 25[1] (2024) 79-84.
27. T. Sato and M. Shimada, Am. Ceram. Soc. Bull. (United States) 64[10] (1985) 6242528.
28. K. Tsacuma, Amer. Ceram. Soc. Bull. 12 (1985) 1594-1596.
29. K. Tsukuma and M. Shimada J. Mater. Sci. 20 (1985) 1178-1184.
30. A. Shelyug and A. Navrotsky, Journal of Nuclear Materials 517 (2019) 80-85.
31. J. Wang, M. Chen, Y. Xu, L. Chen, Y. Yu, J. Sun, Y.

- Wang, B. Liu, and Q. Jing, *Ceram. Int.* 47[23] (2021) 32874-32881.
32. A. Senapati, S.K. Barik, P.K. Parida, K.K. Madapu, S. Balakrishnan, H. Jena, and S.K. Dhara *Ceram. Int.* 49[24] (2023) 40716-40728.
33. M. Abolfazli and M.H. Paydar, *J. Ceram. Process. Res.* 23[2] (2022) 188-198.
34. N.A. Rejab, A.Z.A. Azhar, M.M. Ratnam, and Z.A. Ahmad, *Int. J. Refract. Hard Met.* 36 (2013) 162-166.
35. R.C. Garvie, *J. Phys. Chem.* 69[4] (1965) 1238-1243.
36. N. Claussen, *J. Am. Ceram. Soc.* 59[1-2] (1976) 49-51.